

# Automatic Detection of Eye Cataract using Deep Convolution Neural Networks (DCNNs)

Md. Rajib Hossain

*Dept. of Computer Science & Engineering  
Chittagong University of Engineering & Technology  
Chittagong, Bangladesh  
e-mail: rajcsecuet@gmail.com*

Nazmul Siddique

*School of Computing, Engineering & Intelligent Systems  
Ulster University  
United Kingdom  
e-mail: nh.siddique@ulster.ac.uk*

Sadia Afroze

*Dept. of Computer Science & Engineering  
Chittagong University of Engineering & Technology  
Chittagong, Bangladesh  
e-mail: sadiacse10@gmail.com*

Mohammed Moshiul Hoque

*Dept. of Computer Science & Engineering  
Chittagong University of Engineering & Technology  
Chittagong, Bangladesh  
e-mail: mmoshiulh@gmail.com*

**Abstract**—Eye cataract is a condition in which the lens of the eye becomes clouding or less transparent. This affects the clear vision and is the most prevailing causes of blindness. Therefore, early cataract detection and prevention may reduce the blindness rate and surgery pain of the patients. This paper presents an eye cataract detection system using Deep Convolution Neural Network (DCNNs) comprising two modules: training and testing. The proposed DCNNs architecture is trained, validated and tested with retinal fundus images. Experimental result shows that the proposed system is capable of detecting eye cataract with high accuracy.

**Index Terms**—Medical imaging, Cataract detection, Local feature extraction, Residual networks, Image processing

## I. INTRODUCTION

Eyes are the unique vision gland in the human body and many people are suffering from eye disorder causing vision impairments. Cataract is one of the most prevalent eye diseases which is the frequent reason for blindness. Fig. 1 shows a retinal fundus image which represents the normal retinal fundus image that visible the capillaries and vascular cell (Fig. 1a). Fig. 1b shows a cataract image in which capillaries and vascular are not visible due to blurriness. At this stage, vision is lost in most of the people.

According to the World Health Organization (WHO), at least 2.2 billion people around the world are affected by blindness and vision impairments, around 1 billion people have preventable vision impairments, more than 50% of the blindness is caused by cataract and around 40 million people will be blind by the year 2025 [1]–[3]. Early detection and diagnosis may degrade the lamenting of cataract complaints and prevent visual impairment from turning into blindness. In Bangladesh, more than 750000 people are blind among which 80% are blind due to cataract. People living in the rural and remote areas are the most affected by blindness

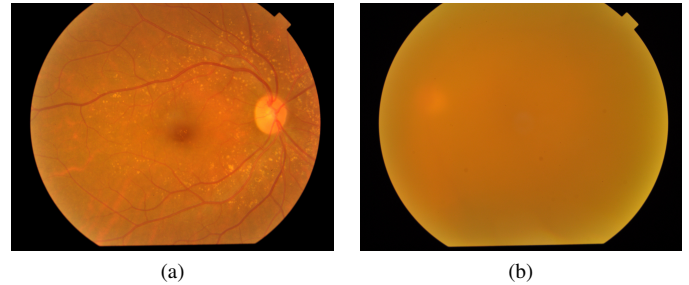


Fig. 1. Retinal Fundus Image (a) non-cataract (b) cataract

due to inaccessibility to health services and ophthalmologists. An intelligent digital eye cataract detection system would be very useful and affordable for those people. Therefore, the develop of an intelligent eye cataract detection system has been a research focus for some time. In the recent years, many electronics devices have developed for retinal fundus image capturing and detecting cataract but these devices are reported to be expensive and have poor ability of detecting cataract. As a result, there is a need for the development of a low-cost computer-assisted intelligent cataract detection system that will reduce the dependency on ophthalmologists or similar eye specialist for eye treatment such as cataract detection. This paper proposed an automatic cataract detection system based on DCNNs that detect the cataract and non-cataract from retinal fundus images. A trained classifier model based on Res-Net [5] is used for the cataract detection.

The rest of the paper is organized as follows: Section II presents related work. Section III presents the methodology. Experiments are presented in Section IV. Section V describes the results. The conclusion is presented in Section VI.

## II. RELATED WORK

There are many statistical approaches developed for cataract detection, but these approaches do not provide satisfactory results due to the limitations of feature extraction and pre-processing. Li et al. [7] developed a cataract detection system based on a 2D Gaussian filter and decision tree algorithm trained by 1355 retinal fundus images, which achieved an accuracy of 92.8%.

But the decision tree is not capable of working with high dimension images. The deep convolution neural network-based approach trained by 5620 images achieved an accuracy of 93.52% but this work failed to manage the vanishing gradient problem [8]. Budai et al. [9] introduced a traditional machine learning-based approach such as support vector machine (SVM). In this system, the whole image is segmented into 17 parts and each part feed to the SVM system. This approach obtained an accuracy of 87.52% but the partial cataract is not detected by their system. Smartphones with OpenCV libraries are used for cataract detection , but it was experimented only on 70 images that achieved an accuracy of 90.00% [10].

A DCNN with a random forest-based cataract classifier model has been reported by Ran et al. [11]. They trained the cataract detection system with 3460 retinal fundus images and tested on 1948 images achieving an accuracy of 97.04%. A recent work used an active shape model with SVM which trained on more than 5000 images and achieved an accuracy of 95.00% [12]. The SVM kernel is not able to train high dimension feature map. Principle component analysis (PCA) and the wavelet technique are applied to cataract detection and grading purposes [13]. Most of the previous research inferred that the statistical learning algorithm (SVM, decision tree, active shape model, random forest, etc.) requires prior training knowledge and not able to train high dimension features. The DCNN and other recent approaches are not able to overcome the overfitting and underfitting problems due to layer design. Zhou et al. [22] developed a discrete state transition (DST) and Res-Net based system. They have achieved the best cataract detection performance (94.00%) and overcome the vanishing gradient problems. The proposed DCNNs architecture overcomes the vanishing gradient problems using the residual connection technique. It also eliminates the image pre-processing step and able to propagates high dimension features. The DCNN architecture can capture deep semantic features from retinal fundus images and represent a high accuracy classifier model.

## III. METHODOLOGY

This study proposes an automatic cataract detection system that consists of two key modules: training and testing. Fig. 2 shows the architecture of the proposed cataract detection system. The training module trained with labeled data sets using the DCNNs classifier algorithm. The testing module tests unlabeled data.

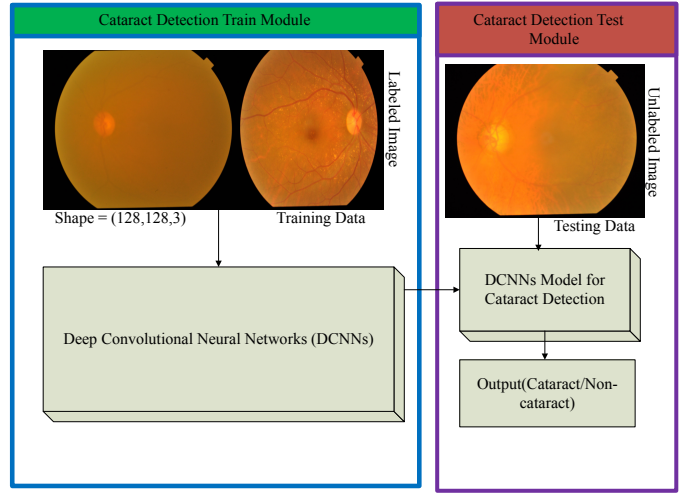


Fig. 2. Cataract detection DCNNs architecture

### A. Training Module

Cataract detection train module is implemented using a supervised DCNNs algorithm. This module is a detection model with Res-Net50 [5] like architecture that detects the cataract and non-cataract retinal fundus images. The training labeled data sets ( $D = (x_1, y_1), (x_2, y_2), (x_3, y_3) \dots (x_n, y_n)$ ), where pair  $(x_i, y_i)$  indicates the input image with labeled data and  $n$  represent the total number of labeled data in the training system. The labeled  $y_i \in C$ , where  $C$  is the class number. For detection purpose  $C = 2$ .

Res-Net50 has consisted of five stages. The first stage contains a convolution, batch normalization, activation, and max-pooling layers. The second stage consists of a single convolution block and two identity blocks. The third stage has one convolution block and three identity blocks. The fourth stage has a convolution block and five identity blocks. At the last stage compress a convolution block and two identity blocks. In this architecture, our cataract dataset generates an overfitted detection model due to a shortage of datasets. In the DCNNs system, inherit from the Res-Net50 layer architecture with a few changes in each of the stage which overcome the overfitting problems. Input layer start with an input retinal fundus image shape (128, 128, 3), where 128 height and width and 3 indicate the image depth and connect to zero padding that convert to shape (134, 134, 3). The input propagates through five stages of layered-architecture. The first stage comprises follows convolution (Conv2D), batch normalization [6] (BN), activation and max-pooling layer. The second stage starts with convolution block followed by two identity blocks. The identity blocks also contain three levels of convolution operations with the input and output remained the same. The third stage comprises a single convolution block and an identity block. The fourth stage block has a convolution block and an identity block. At the fifth stage, the convolution block is followed by an identity block. Average pooling is used imposed for feature reduction purpose at the end of stage five

and flattened the high dimensional feature space. The dense layer is followed by a fully connected layer. The convolution operation carried out using Eq. [6].

$$I(i, j) = \sum_{i=0}^{I_h} \sum_{j=0}^{I_w} \sum_{k=0}^{K_h} \sum_{l=0}^{K_w} I(i+k, j+l) \times K(k, l) \quad (1)$$

Here, the input position  $I(i, j)$  extract the local feature according to operation  $I(i+k, j+l) \times K(k, l)$ , where  $K(k, l)$  is the kernel or trainable weights filter. The convolution operation mainly extracts the local feature and helps to train the weights filter. The batch normalization reduces the training time and helps pre-processing the feature value. It also controls the model overfitting. Batch normalization operations are performed using Eqs. (2)-(4).

$$\mu_I = \frac{1}{N} \sum_{j=1}^N I_j \quad (2)$$

$$\sigma_I^2 = \frac{1}{N} \sum_{j=1}^N (I_j - \mu_I) \times (I_j - \mu_I) \quad (3)$$

$$\hat{I}_f^i = \frac{I_f^i - \mu_I}{\sqrt{\sigma_I^2 + \epsilon}} \quad (4)$$

Here,  $\mu_I$ ,  $\sigma_I^2$  and  $\hat{I}_f^i$  represent the input feature mean, standard deviation and normalize features value respectively. In the proposed layer design, each stage has a batch normalization operation and followed by the convolution operation. The batch normalization operation improves the gradient calculation operation and reduces the time complexity. After the batch normalization operation, an activation operation is applied to the feature space (Eq. 5).

$$I(i, j) = \max(I(i, j), 0) \quad (5)$$

In this operation, all the negative feature values are replaced by zero (0). Activation operation reduces the solution converge time and acts as a feature normalization function. Two types of pooling operations have been used in DCNN architecture. These are max pooling and average pooling. The 2D max-pooling operation reduces the feature map space and model overfitting problem. The 2D average-pooling operation averages the square size feature value. The detection loss of DCNN architecture is calculated using 6.

$$L(I) = - \sum_{i=0}^C S_i \times \log(p_i) \quad (6)$$

Here, the  $L(I)$ ,  $S_i$  and  $p_i$  are the loss value for feature  $I$ , true labeled for  $i^{th}$  sample and probability of that sample respectively. For the detection purpose, the  $C$  is 2. The negative sign uses to revert the log value sign. After completing all the processes, the DCNNs algorithm generates a cataract detection model. The cataract detection model is a binary classifier.

## B. Testing Module

In the testing module, unlabeled image data are input. Then the module detects if the images have cataracts or not using DCNNs model. The trainable parameters of DCNNs are initialized by the cataract detection value. The parameters of the convolution layer and fully connected layer only extract the feature from the learned parameters. The Soft-max layer or output layer determines the expected value using Eq. 7.

$$E_x = \sum_{i=0}^C \sum_{j=0}^{F_d} I(i, j) \times W(i, j) \quad (7)$$

Here,  $E_x$  is the expected value. For detection, it returns two values. Weights matrix  $W(i, j)$  is the soft-max layer and  $I(i, j)$  refers to input feature map. The soft-max score is calculated for detection using Eq. 8.

$$P(E_x|y_x) = \frac{e^{E_x}}{\sum_{i=0}^C e^{E_{x_i}}} \quad (8)$$

Here,  $P(E_x|y_x)$  has two scores for cataract detection. The  $\max(P(E_x|y_x))$  returns the maximum value index of the detection model. For the detection model, zero index indicates non-cataract and one index indicates the cataract.

## IV. EXPERIMENTS

The proposed DCNN cataract detection system is implemented using Keras deep learning library with TensorFlow back end [23]. The designed system runs on an NVIDIA GTX 1070 GPU with 32 GB RAM, Intel i7-7700K (LGA-1151) 7TH GEN, 4.20GHZ processor and Ubuntu16.04 operating system.

### A. Dataset

The retinal fundus images are collected from several eye hospitals in Bangladesh (cataract=3000) and some open-access datasets (non-cataract=1000). The high-resolution fundus (HRF) image database [15] contains some retinal images, that are used for a non-cataract class (non-cataract=40, cataract=5). The digital retinal images from vessel extraction (DRIVE) [17] database are used for retinal vessel segmentation purposes (non-cataract=40). These images are included in the normal and cataract category data set. The structure analysis of retina (STARE) [16] images database included as a non-cataract category (non-cataract = 380, cataract = 17). Indian diabetic retinopathy image dataset (IDRiD) [18] contains the severe, mild, moderate and normal stage cataract images (non-cataract=490, cataract=26). The data sets have been prepared for training, validation and testing purposes. Table I illustrates the cataract detection data sets summary. The retinal fundus image considers as non-cataract category and remaining all images are considered as cataract categories. So, the total number of non-cataract category images is about 2670 and the number of cataract images is nearly 3048.

TABLE I  
RETINAL FUNDUS IMAGE DATA SUMMARY

Category Name	#Training images	# Validation images	#Testing images
Cataract	2000	150	898
Non-cataract	2000	150	520
Total	4000	300	1418

### B. Evaluation Measures

The proposed DCNN based cataract detection system is evaluated in two phases. The training and validation phase loss values are calculated using Eq. 6. The accuracy is calculated from the actual and predicted labeled using these ratios  $\frac{\#actual\_predict}{\#sample}$ . Actual prediction value is calculated from the ground truth and the predicted value. The testing phase evaluation is performed using some statistical measures. The ground truth cataract properly detected as cataract is called true positive ( $(T_p)$ ) and incorrectly detected as positive is called false positive ( $F_p$ ). The ground truth negatively labeled cataract detected as negative is called true negative ( $T_n$ ) and incorrectly detected as negative is called false negative ( $F_n$ ). Now, the sensitivity ( $S_t$ ), specificity ( $S_f$ ), true positive rate ( $TPR$ ), false positive rate ( $FPR$ ), Error rate ( $ERR$ ) and accuracy ( $A$ ) are calculated according to Eqs. (9-16) [24].

$$S_t = \frac{T_p}{T_p + F_n} \quad (9)$$

$$S_f = \frac{T_n}{T_n + F_p} \quad (10)$$

$$TPR = \frac{T_p}{T_p + F_n} \quad (11)$$

$$FPR = \frac{F_p}{F_p + T_n} \quad (12)$$

$$A = \frac{T_p + T_n}{T_p + T_n + F_p + F_n} \quad (13)$$

$$Precision(P) = \frac{T_p}{T_p + F_n} \quad (14)$$

$$Recall(R) = \frac{T_p}{T_p + F_p} \quad (15)$$

$$ERR = \frac{F_p + F_n}{T_p + T_n + F_p + F_n} \quad (16)$$

The **confusion matrix** is represented by a  $2 \times 2$  matrix in which the diagonal cells indicate the actual predicted values by the system and the other cells indicate the incorrectly predicted values [25].

### V. RESULTS

In Fig. 3 shows the cataract detection accuracy. In the cataract detection system, training and validation accuracy start from 0.81 and 0.86 respectively. After two epochs, the training and validation accuracy gradually increases. At epoch 10 and onwards, the accuracy becomes stable for training and validation sets. The training accuracy reaches close to 100.00% from epoch 15 and onwards and validation accuracy reaches close to 97.38%. The visual representation in Fig. 3 concludes that the model of cataract detection system does not overfitted and underfitted according to training and validation accuracy. The cataract detection loss in the training and

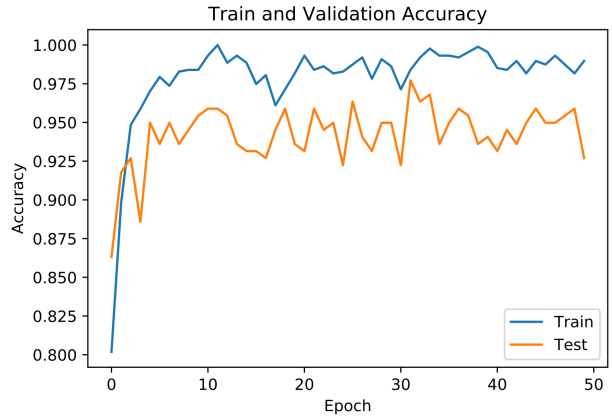


Fig. 3. Cataract detection training and validation accuracy.

validation phases is presented in Fig. 4. The training loss begins from 2.25 average logarithmic loss value where the validation loss value is 0.25. After some few epochs, the training and validation loss are almost fixed. At epochs from 11 to 45 the training and validation loss curves progressively preserve a stable distance. These graphical illustrations of the detection loss during the training and validation phase infer that the model is neither overfitting nor underfitting

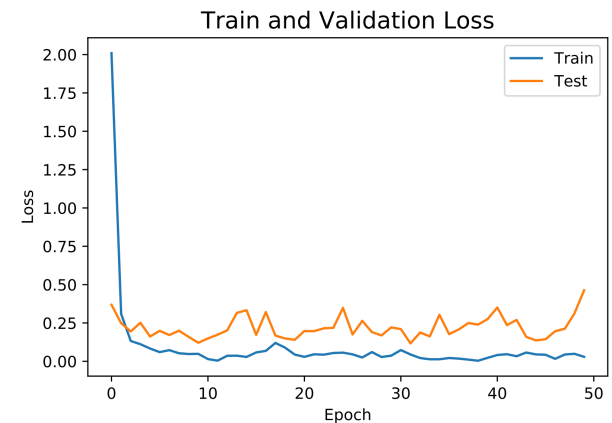


Fig. 4. Cataract detection training and validation loss.

Fig. 5 shows the graphical representation of the cataract detection Receiver Operating Characteristic (ROC) curve. In classification the ROC curve measures the best threshold value for cataract and non-cataract, which is found at 0.97. That means, the classifier predicted score below the threshold value is considered as non-cataract and above the threshold value is considered as the cataract stage. The diagonal line represents random threshold value, which is 0.50. The Area Under the Curve (AUC) value measures the model performance and the relativity between the training and test dataset. Fig. 5 shows that the AUC value is 0.982 which is indicated by the lower part of the blue curve.

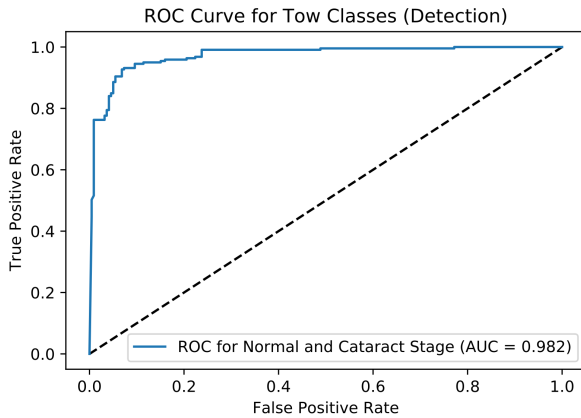


Fig. 5. Cataract detection ROC curve.

The confusion matrix is shown in Table II. The first diagonal value of 848 indicates the correctly classified cataract and 50 incorrectly classified retinal fundus images by the DCNN system. The second diagonal value is 510, which indicates the DCNN system can precisely predict non-cataract and inaccurately predict 10 images. The confusion matrix also

TABLE II  
CONFUSION MATRIX FOR CATARACT DETECTION

		Predicted		Total
		Cataract	Non-cataract	
Actual	Cataract	848	50	898
	Non-cataract	10	510	520
Total		858	560	

implies that the DCNN system incorrectly detected 50 cataract images as non-cataract due to retinal vessel clarity. The mild stage cataract retinal images look like non-cataract images and these images are not detected by the DCNN system. The number of non-cataract images that are incorrectly predicted as cataract images is low. There are only 10 images that could not be predicted by the DCNN system.

Table III shows the different types of statistical outcomes of the DCNN system. Sensitivity or cataract samples predicted as cataract is the model fitness. The specificity or the non-cataract samples predicted as non-cataract is the individual class accuracy. In this research, the specificity achieved is

98.07%, which is the best accuracy compared to previously published results. The overall DCNN system accuracy is

TABLE III  
STATISTICAL MEASUREMENTS FOR CATARACT DETECTION

Cataract Detection	Result(%)
Sensitivity ( $S_t$ )	94.43
Specificity ( $S_f$ )	98.07
Accuracy (A)	95.77
Precision (P)	94.43
Recall (R)	98.83
Error rate (ERR)	4.23

95.77% and the error rate is 4.23%. Some of the retinal fundus images contain partial cataract, which cause confusion. But the overall measurement shows that the DCNN system is not overfitted or underfitted.

Table IV shows the accuracy comparison between human expertise vs DCNN system. Four ophthalmic experts voted for each image like cataract or non-cataract. Finally, the maximum number of votes ensured the category name (cataract or non-cataract). In this way, we evaluated 1418 retinal fundus images by the ophthalmic experts and finally calculated the average sensitivity and specificity.

TABLE IV  
HUMAN VS DCNNs SENSITIVITY AND SPECIFICITY

Category Name	Human (%)	DCNNs (%)
Specificity ( $S_f$ )	100.00	98.07
Sensitivity ( $S_t$ )	98.00	94.43
Avg.	99.00	96.25

The maximum human experts' specificity is 100.00% where the proposed DCNN system achieved an specificity of 98.07. The overall average sensitivity and specificity by human experts is 99.00% and by the proposed DCNN system is 96.25%.

Table V shows the comparison between the proposed DCNNs and previous approaches. Lvchen et al. [19] are used the Haar-wavelet technique and achieved 94.83% accuracy. Discrete state transition (DST) with Res-Net [12] based system

TABLE V  
CATARACT DETECTION ACCURACY COMPARISON

Algorithm Name (Year)	#Training/Validation Images	#Testing Images	Accuracy(%)
Hierarchical+Haar-wavelet [19] (2019)	1300	-	94.83
BPNN [20] (2013)	-	-	90.86
Fourier analysis [21] (2008)	330	-	61.9
DST-ResNet [22] (2020)	1355/350	350	94.00
<b>Proposed(DCNNs)</b>	<b>4000/300</b>	<b>1418</b>	<b>95.77</b>

has achieved 94.00% accuracy on test dataset (350). The proposed DCNNs has gained a better accuracy (about 95.77%) than the previous approaches.

## VI. CONCLUSION

An automatic cataract detection system using DCNN architecture is proposed in this work. The proposed system obtained

an accuracy of 95.77% on test sets. The proposed DCNN system overcomes the traditional feature extraction limitations and this system has no requirement for image pre-processing. The graphical and statistical results show that the proposed system additionally overcomes the model overfitting and underfitting issues. The proposed system may be incorporated into internet of things (IoT) device which may be of great help for ophthalmologists. The proposed system is cheaper and can be easily used by the rural/low income peoples to ensure better cataract treatment service. The proposed system is unable to detect the partial or mild cataract in retinal fundus images. Detection of mild stage or partial cataract is left for a future study and development of the DCNNs system.

## REFERENCES

- [1] D. Allen and A. Vasavada, "Cataract and surgery for cataract," *BMJ*, vol. 333, no. 7559, pp. 128–132, Jul. 2006.
- [2] A. Foster, Ed., "Vision 2020: the cataract challenge," *Community eye Heal.*, vol. 13, no. 34, pp. 17–19, 2000.
- [3] D. Pascolini and S. P. Mariotti, "Global estimates of visual impairment: 2010," *Br. J. Ophthalmol.*, vol. 96, no. 5, pp. 614–618, 2012.
- [4] T. Pratap and P. Kokil, "Computer-aided diagnosis of cataract using deep transfer learning," *Biomedical Signal Processing and Control.*, vol. 53, Aug. 2019.
- [5] K. He, X. Zhang, S. Ren and J. Sun, "Deep Residual Learning for Image Recognition," 2016 IEEE Conference on Computer Vision and Pattern Recognition (CVPR), pp. 770-778, Las Vegas, NV, 2016.
- [6] S. Ioffe and C. Szegedy, "Batch normalization: accelerating deep network training by reducing internal covariate shift," *International Conference on Machine Learning*, Vol. 37, pp. 448-456, 2015.
- [7] L. Xiong, H. Li, and L. Xu, "An Approach to Evaluate Blurriness in Retinal Images with Vitreous Opacity for Cataract Diagnosis," *J. Healthc. Eng.*, vol. 2017, 2017.
- [8] Linglin Zhang et al., "Automatic cataract detection and grading using Deep Convolutional Neural Network," 2017 IEEE 14th International Conference on Networking, Sensing and Control (ICNSC), Calabria, 2017, pp. 60-65.
- [9] Z. Qiao, Q. Zhang, Y. Dong and J. Yang, "Application of SVM based on genetic algorithm in classification of cataract fundus images," 2017 IEEE International Conference on Imaging Systems and Techniques (IST), Beijing, 2017, pp. 1-5.
- [10] J. Rana and S. M. Galib, "Cataract detection using smartphone," 2017 3rd International Conference on Electrical Information and Communication Technology (EICT), Khulna, 2017, pp. 1-4.
- [11] J. Ran, K. Niu, Z. He, H. Zhang and H. Song, "Cataract Detection and Grading Based on Combination of Deep Convolutional Neural Network and Random Forests," 2018 International Conference on Network Infrastructure and Digital Content (IC-NIDC), Guiyang, 2018, pp. 155-159.
- [12] H. Li et al., "A Computer-Aided Diagnosis System of Nuclear Cataract," in *IEEE Transactions on Biomedical Engineering*, vol. 57, no. 7, pp. 1690-1698, July 2010.
- [13] W. Fan, R. Shen, Q. Zhang, J.-J. Yang, and J. Li, "Principal component analysis based cataract grading and classification," in 2015 17th International Conference on E-health Networking, Application & Services (HealthCom), 2015, pp. 459–462.
- [14] H. Shin et al., "Deep Convolutional Neural Networks for Computer-Aided Detection: CNN Architectures, Dataset Characteristics and Transfer Learning," in *IEEE Transactions on Medical Imaging*, vol. 35, no. 5, pp. 1285-1298, May 2016.
- [15] A. Budai, R. Bock, A. Maier, J. Hornegger, G. Michelson, "Robust vessel segmentation in fundus images," *Int. J. Biomed. Imaging* (2013), Article ID 154860, 2013.
- [16] A. D. Hoover, V. Kouznetsova and M. Goldbaum, "Locating blood vessels in retinal images by piecewise threshold probing of a matched filter response," in *IEEE Transactions on Medical Imaging*, vol. 19, no. 3, pp. 203-210, March 2000.
- [17] J. Staal, M. D. Abramoff, M. Niemeijer, M. A. Viergever and B. van Ginneken, "Ridge-based vessel segmentation in color images of the retina," in *IEEE Transactions on Medical Imaging*, vol. 23, no. 4, pp. 501-509, April 2004.
- [18] P. Porwal, S. Pachade, R. Kamble, M. Kokare, G. Deshmukh, V. Sahasrabuddhe and F. Meriaudeau, "Indian Diabetic Retinopathy Image Dataset (IDRiD)," *IEEE DataPort*, 2018.
- [19] L. Z. Lvchen Cao, Huiqi Li, Yanjun Zhang, Liang Xu, "Hierarchical method for cataract grading based on retinal images using improved Haar wavelet," *arXiv Prepr. arXiv1904.01261*, 2019.
- [20] M. Yang, J.-J. Yang, Q. Zhang, Y. Niu, and J. Li, "Classification of retinal image for automatic cataract detection," in 2013 IEEE 15th International Conference on e-Health Networking, Applications and Services (Healthcom 2013), 2013, pp. 674–679.
- [21] A. M. Abdul-Rahman, T. Molteno, and A. C. B. Molteno, "Fourier analysis of digital retinal images in estimation of cataract severity," *Clin. Experiment. Ophthalmol.*, vol. 36, no. 7, pp. 637–645, 2008.
- [22] Y. Zhou, G. Li and H. Li, "Automatic Cataract Classification Using Deep Neural Network With Discrete State Transition," in *IEEE Transactions on Medical Imaging*, vol. 39, no. 2, pp. 436-446, Feb. 2020.
- [23] F. Chollet, "Keras," [Online]. Available: <https://github.com/keras-team/keras>, 2015.
- [24] Wikipedia, "Precision and recall," Last modified 28 February 2020, [Online]. Available: [https://en.wikipedia.org/wiki/Precision\\_and\\_recall](https://en.wikipedia.org/wiki/Precision_and_recall)
- [25] Wikipedia, "Confusion Matrix," Last modified 11 February 2020, [Online]. Available: [https://en.wikipedia.org/wiki/Confusion\\_matrix](https://en.wikipedia.org/wiki/Confusion_matrix)